

Activation of Atmospheric Nitrogen and Azobenzene N=N Bond Cleavage by a Transient Nb(III) Complex

Uriah J. Kilgore, Xiaofan Yang, John Tomaszewski, John C. Huffman, and Daniel J. Mindiola*

Department of Chemistry and Molecular Structure Center, Indiana University, Bloomington, Indiana 47405

Received August 30, 2006

Atmospheric N₂ is activated by two transient Nb(III) "(PNP)NbCl₂" (PNP⁻ = N[2-P(CHMe₂)₂-4-methylphenyl]₂) fragments to form the bridging diimido [(PNP)NbCl₂]₂(μ-N₂) (**1**). Complex **1** can also be independently synthesized from Nb(IV) and Nb(V) precursors via one-electron and transmetalation reactions, respectively. In the presence of azobenzene, the transient Nb(III) intermediate, prepared from Li(PNP) and NbCl₃(DME) (DME = dimethoxyethane) under Ar, cleaves the N=N bond via a metal–ligand cooperative four-electron reduction to form niobium imide and phosphoranime functionalities. Structural studies are presented and discussed for various Nb systems bearing the pincer-type framework PNP as well as the N₂ and azobenzene activated products. Theoretical studies addressing the Nb–N₂–Nb core in **1** are also presented.

Introduction

Despite it being a mature field, organotransition-metal chemistry involving activation and functionalization of atmospheric N₂ still continues to draw attention given its relevance to both nitrogenases¹ and the Haber–Bosch process.² Consequently, the significance of the N₂ cycle places systems that are capable of activating and/or functionalizing N₂ in a category of widespread interest. One common practice for activating atmospheric N₂ involves the generation of powerful π bases, in particular unsaturated and low-valent metal complexes capable of backbonding into the high-energy N₂ π* orbitals.³ Typically, the low-valent metal center in question can be generated from a masked low-coordinate synthon,⁴ as a sterically protected mononuclear

metal complex with an open coordination for the small substrate,^{3a,5} or by using powerful reductants such as the alkali metals or hydrides.^{3,6} The latter type of reaction appears to be the most common procedure to activate N₂. Hence, N₂ can act as a trapping substrate (in situ) for the electron-rich metal fragment and thus limit its propensity to undergo decomposition. However, activating N₂ using low-valent metal halide precursors, and in the absence of external stimulants such as powerful reductants, is a rare phenomenon in the context of organotransition-metal chemistry.^{7,8}

In this work, we report the activation of atmospheric N₂ by two transient Nb(III) molecules to afford a topologically linear Nb=N=N=Nb core. Synthesis of the dinuclear N₂ complex can be accomplished through three independent routes that involve Nb(III), Nb(IV), and Nb(V) precursors. In addition to N₂ activation, we also report the four-electron reductive cleavage of azobenzene, in a cooperative fashion, by Nb(III) and P(III) centers.

Recent work with the pincer-type ligand PNP (PNP⁻ = N[2-P(CHMe₂)₂-4-methylphenyl]₂)⁹ has shown this to be a

* To whom correspondence should be addressed. E-mail: mindiola@indiana.edu.

- (1) (a) Howard, J. B.; Rees, D. C. *Chem. Rev.* **1996**, *96*, 2965–2982. (b) Burgess, B. K.; Lowe, D. J. *Chem. Rev.* **1996**, *96*, 2983–3011.
- (2) (a) Stoltzenberg, D. *Fritz Haber. Chemist, Nobel laureate, German, Jew*; Chemical Heritage Press: Philadelphia, PA, 2004. (b) Appl, M. *Ammonia*; Wiley-VCH: Weinheim, Germany, 1999.
- (3) For some recent reviews on N₂ activation by transition metals, see: (a) Schrock, R. R. *Acc. Chem. Res.* **2005**, *38*, 955–962. (b) Leigh, G. J. *Acc. Chem. Res.* **1992**, *25*, 177–181. (c) MacKay, B. A.; Fryzuk, M. D. *Chem. Rev.* **2004**, *104*, 385–402. (d) Hidai, M.; Mizobe, Y. *Chem. Rev.* **1995**, *95*, 1115–1133. (e) Hidai, M. *Coord. Chem. Rev.* **1999**, *185–186*, 99–108. (f) Gambarotta, S. *J. Organomet. Chem.* **1995**, *500*, 117–126. (g) Fryzuk, M. D.; Johnson, S. A. *Coord. Chem. Rev.* **2000**, *200–202*, 379–409. (h) Gambarotta, S.; Scott, J. *Angew. Chem., Int. Ed.* **2004**, *43*, 5298–5308. (i) MacLachlan, E. A.; Fryzuk, M. D. *Organometallics* **2006**, *25*, 1530–1543. (j) Shaver, M. P.; Fryzuk, M. D. *Adv. Synth. Catal.* **2003**, *345*, 1061–1076.

- (4) (a) Tsai, Y.-C.; Johnson, M. J. A.; Mindiola, D. J.; Cummins, C. C.; Klooster, W. T.; Koetzle, T. F. *J. Am. Chem. Soc.* **1999**, *121*, 10426–10427. (b) Gao, Y.; Holah, D. G.; Hughes, A. N.; Spivak, G. J.; Havighurst, M. D.; Magnuson, V. R. *Polyhedron* **1998**, *17*, 3881–3888. (c) King, W. A.; Scott, B. L.; Eckert, J.; Kubas, G. J. *Inorg. Chem.* **1999**, *38*, 1069–1084. (d) Hammer, R.; Klein, H.-F.; Schubert, U.; Frank, A.; Huttner, G. *Angew. Chem., Int. Ed. Engl.* **1976**, *15*, 612–613. (e) Fout, R.; Basuli, F.; Fan, H.; Tomaszewski, J.; Huffman, J. C.; Baik, M.-H.; Mindiola, D. J. *Angew. Chem., Int. Ed.* **2006**, *45*, 3291–3295.

robust ancillary support for Ti complexes bearing terminal phosphinidene,¹⁰ alkylidene,^{10,11} and alkylidyne¹² frameworks. In addition, the PNP scaffold has shown itself to be an excellent platform for the stabilization of low-valent late transition metals such as Co(I) and Co(1-).¹³ Inadvertently, these two Co complexes have been implicated in the sequestration of atmospheric N₂. Given the latter precedent and the fact that low-valent Nb complexes can activate

N₂,^{8f,h,14} we speculated whether the PNP framework would be appropriate in stabilizing a powerful reductant such as a rare and monomeric Nb(III) complex “(PNP)NbCl₂”.¹⁵

Experimental Section

General Considerations. Unless otherwise stated, all operations were performed in a M. Braun Lab Master double drybox under an atmosphere of purified N₂ or using high-vacuum standard Schlenk techniques under an Ar atmosphere.¹⁶ Anhydrous *n*-hexane, pentane, toluene, and benzene were purchased from Aldrich in sure-sealed reservoirs (18 L) and dried by passage through two columns of activated alumina and a Q-5 column.¹⁷ Diethyl ether (DME) and CH₂Cl₂ were dried by passage through two columns of activated alumina.¹⁷ Tetrahydrofuran (THF) was distilled, under N₂, from purple sodium benzophenone ketyl and stored under Na metal. Distilled THF was transferred under vacuum into bombs before being pumped into a drybox. C₆D₆ and CD₂Cl₂ were purchased from Cambridge Isotope Laboratory, degassed and dried over CaH₂, and then vacuum transferred to 4-Å molecular sieves. Celite, alumina, and 4-Å molecular sieves were activated under vacuum overnight at 200 °C. Li(PNP),⁹ NbCl₃(DME),¹⁸ NbCl₄(THF)₂,¹⁹ [NbCl₃(THF)₂]₂(μ-N₂),²⁰ KC₈,²¹ and Mg(THF)₃(anthracene)²² were prepared according to the literature. CHN analyses were performed by Desert Analytics, Tucson, AZ. ¹H and ¹³C{¹H} NMR spectra were recorded on Varian 400- or 300-MHz NMR spectrometers. ¹H and ¹³C{¹H} NMR spectra are reported with reference to solvent resonances (residual C₆D₅H in C₆D₆, 7.16 and 128.0 ppm). ⁹³Nb and ¹⁵N NMR spectra were recorded on a Varian INOVA 500-MHz spectrometer with reference to CH₃NO₂ at 380 ppm and NbCl₅ in C₆D₆ at 0 ppm, respectively.²³ Solution magnetic moment

- (5) (a) Odom, A. L.; Arnold, P. L.; Cummins, C. C. *J. Am. Chem. Soc.* **1998**, *120*, 5836–5837. (b) Laplaza, C. E.; Johnson, A. R.; Cummins, C. C. *J. Am. Chem. Soc.* **1996**, *118*, 709–710. (c) Mendiola, D. J.; Meyer, K.; Cherry, J.-P. F.; Baker, T. A.; Cummins, C. C. *Organometallics* **2000**, *19*, 1622–1624. (d) Peters, J. C.; Cherry, J.-P. F.; Thomas, J. C.; Baraldo, L.; Mendiola, D. J.; Davis, W. M.; Cummins, C. C. *J. Am. Chem. Soc.* **1999**, *121*, 10053–10067. (e) Laplaza, C. E.; Johnson, M. J. A.; Peters, J. C.; Odom, A. L.; Kim, E.; Cummins, C. C.; George, G. N.; Pickering, I. J. *J. Am. Chem. Soc.* **1996**, *118*, 8623–8638. (f) Laplaza, C. E.; Cummins, C. C. *Science* **1995**, *268*, 861–863. (g) O'Donoghue, M. B.; Zanetti, N. C.; Davis, W. M.; Schrock, R. R. *J. Am. Chem. Soc.* **1997**, *119*, 2753–2754. (h) Yandulov, D. V.; Schrock, R. R. *J. Am. Chem. Soc.* **2002**, *124*, 6252–6253. (i) Shih, K.-Y.; Richard, R.; Schrock, R. R.; Kempe, R. *J. Am. Chem. Soc.* **1994**, *116*, 8804–8805. (j) O'Donoghue, M. B.; Davis, W. M.; Schrock, R. R.; Reiff, W. M. *Inorg. Chem.* **1999**, *38*, 243–252. (k) Yandulov, D. V.; Schrock, R. R. *Inorg. Chem.* **2005**, *44*, 1103–1117. (l) Ritleng, V.; Yandulov, D. V.; Weare, W. W.; Schrock, R. R.; Hock, A. S.; Davis, W. M. *J. Am. Chem. Soc.* **2004**, *126*, 6150–6163. (m) O'Donoghue, M. B.; Davis, W. M.; Schrock, R. R. *Inorg. Chem.* **1998**, *37*, 5149–5158. (n) Greco, G. E.; Schrock, R. R. *Inorg. Chem.* **2001**, *40*, 3861–3878. (o) Kol, M.; Schrock, R. R.; Kempe, R.; Davis, W. M. *J. Am. Chem. Soc.* **1994**, *116*, 4382–4390. (p) Murahashi, T.; Clough, C. R.; Figueroa, J. S.; Cummins, C. C. *Angew. Chem., Int. Ed.* **2005**, *44*, 2560–2563. (q) Roussel, P.; Scott, P. *J. Am. Chem. Soc.* **1998**, *120*, 1070–1071. (r) Evans, W. J.; Kozimor, S. A.; Ziller, J. W. *J. Am. Chem. Soc.* **2003**, *125*, 14264–14265. (s) O'Donoghue, M. B.; Schrock, R. R.; Davis, W. M. *Inorg. Chem.* **1998**, *37*, 5149–5158. (t) Figueroa, J. S.; Piro, N. A.; Clough, C. R.; Cummins, C. C. *J. Am. Chem. Soc.* **2006**, *128*, 940–950.
- (6) Examples of N₂ activation promoted by external reductants are extensive. We refer the reader to review articles listed in ref 3.
- (7) N₂ cleavage using light as an energy source has been documented. (a) Solari, E.; Silva, C. D.; Iacono, B.; Hesschenbrouck, J.; Rizzoli, C.; Scopelliti, R.; Carlo Floriani, C. *Angew. Chem., Int. Ed.* **2001**, *40*, 3907–3909. (b) Smith, J. M.; Sadique, A. R.; Cundari, T. R.; Rodgers, K. R.; Lukat-Rodgers, G.; Lachicotte, R. J.; Flaschenriem, C. J.; Vela, J.; Holland, P. L. *J. Am. Chem. Soc.* **2006**, *128*, 756–769.
- (8) For some examples depicting N₂ activation by a low-valent transition-metal halide precursor without an external reductant, see: (a) Duchateau, R.; Gambarotta, S.; Beydoun, N.; Bensimon, C. *J. Am. Chem. Soc.* **1991**, *113*, 8986–8988. (b) Evans, W. J.; Allen, N. T.; Ziller, J. W. *J. Am. Chem. Soc.* **2001**, *123*, 7927–7928. (c) Evans, W. J.; Zucchi, G.; Ziller, J. W. *J. Am. Chem. Soc.* **2003**, *125*, 10–11. (d) Evans, W. J.; Lee, D. S.; Ziller, J. W. *J. Am. Chem. Soc.* **2004**, *126*, 454–455. (e) Evans, W. J.; Allen, N. T.; Joseph, W.; Ziller, J. W. *Angew. Chem., Int. Ed.* **2002**, *41*, 351–361. (f) Fryzuk, M. D.; Johnson, S. A.; Patrick, B. O.; Albinati, A.; Mason, S. A.; Koetzle, T. F. *J. Am. Chem. Soc.* **2001**, *123*, 3960–3973. (g) Dube, T.; Conoci, S.; Gambarotta, S.; Yap, G. P. A.; Vasapollo, G. *Angew. Chem., Int. Ed.* **1999**, *38*, 3657–3659. (h) Fryzuk, M. D.; Kozak, C. M.; Patrick, B. O. *Inorg. Chim. Acta* **2003**, *345*, 53–62.
- (9) (a) Fan, L.; Foxman, B. M.; Ozerov, O. V. *Organometallics* **2004**, *23*, 326–328. (b) Ozerov, O. V.; Guo, C.; Fan, L.; Foxman, B. M. *Organometallics* **2004**, *23*, 5573–5580. (c) Ozerov, O. V.; Guo, C.; Papkov, V. A.; Foxman, B. M. *J. Am. Chem. Soc.* **2004**, *126*, 4792–4793. (d) Fan, L.; Yang, L.; Guo, C.; Foxman, B. M.; Ozerov, O. V. *Organometallics* **2004**, *23*, 4778–4787.
- (10) Bailey, B. C.; Huffman, J. C.; Mendiola, D. J.; Weng, W.; Ozerov, O. V. *Organometallics* **2005**, *24*, 1390–1393.
- (11) Weng, W.; Yang, L.; Foxman, B. M.; Ozerov, O. V. *Organometallics* **2004**, *23*, 4700–4705.
- (12) (a) Bailey, B. C.; Fan, H.; Baum, E. W.; Huffman, J. C.; Baik, M.-H.; Mendiola, D. J. *J. Am. Chem. Soc.* **2005**, *127*, 16016–16017. (b) Bailey, B. C.; Fan, H.; Huffman, J. C.; Baik, M.-H.; Mendiola, D. J. *J. Am. Chem. Soc.* **2006**, *128*, 6798–6799.
- (13) Fout, A. F.; Basuli, F.; Fan, H.; Tomaszewski, J.; Huffman, J. C.; Baik, M.-H.; Mendiola, D. J. *Angew. Chem., Int. Ed.* **2006**, *45*, 3291–3295.
- (14) (a) Berno, P.; Gambarotta, S. *Organometallics* **1995**, *14*, 2159–2161. (b) Caselli, A.; Solari, E.; Scopelliti, R.; Floriani, C.; Re, N.; Rizzoli, C.; Chiesi-Villa, A. *J. Am. Chem. Soc.* **2000**, *122*, 3652–3670. (c) Zanotti-Gerosa, A.; Solari, E.; Giannini, L.; Floriani, C.; Chiesi-Villa, A.; Rizzoli, C. *J. Am. Chem. Soc.* **1998**, *120*, 437–438. (d) Fryzuk, M. D.; Kozak, C. M.; Bowdridge, M. R.; Patrick, B. O.; Rettig, S. J. *J. Am. Chem. Soc.* **2002**, *124*, 8389–8397. (e) Kawaguchi, H.; Matsuo, T. *Angew. Chem., Int. Ed.* **2002**, *41*, 2792–2794. (f) Lemenovskii, D. A.; Baukova, T. V.; Perevalova, E. G.; Nesmeyanov, A. N. *Ser. Khim.* **1976**, *10*, 2404–2405.
- (15) Monomeric Nb(III) complexes are exceedingly rare. (a) Veige, A. S.; Slaughter, L. M.; Lobkovsky, E. B.; Wolczanski, P. T.; Matsunaga, N.; Decker, S. A.; Cundari, T. R. *Inorg. Chem.* **2003**, *42*, 6204–6224. (b) Hirsekorn, K. F.; Veige, A. S.; Wolczanski, P. T. *J. Am. Chem. Soc.* **2006**, *128*, 2192–2193. (c) Kleckley, T. S.; Bennett, J. L.; Wolczanski, P. T.; Lobkovsky, E. B. *J. Am. Chem. Soc.* **1997**, *119*, 247–248. (d) Fryzuk, M. D.; Kozak, C. M.; Bowdridge, M. R.; Jin, W.; Tung, D.; Patrick, B. O.; Rettig, S. J. *Organometallics* **2001**, *20*, 3752–3761. (e) Fryzuk, M. D.; Jafarpour, L.; Rettig, S. J. *Organometallics* **1999**, *18*, 4050–4058.
- (16) For a general description of the equipment and techniques used in carrying out this chemistry, see: Burger, B. J.; Bercaw, J. E. In *Experimental Organometallic Chemistry*; Wayda, A. L., Darensbourg, M. Y., Eds.; ACS Symposium Series 357; American Chemical Society: Washington, DC, 1987; pp 79–98.
- (17) Pangborn, A. B.; Giardello, M. A.; Grubbs, R. H.; Rosen, R. K.; Timmers, F. J. *Organometallics* **1996**, *15*, 1518–1520.
- (18) Roskamp, E. J.; Pederson, S. F. *J. Am. Chem. Soc.* **1987**, *109*, 6551–6553.
- (19) Manzer, L. *Inorg. Chem.* **1977**, *16*, 525–528.
- (20) (a) Rocklage, S. M.; Schrock, R. R. *J. Am. Chem. Soc.* **1982**, *104*, 3077–3081. (b) Dilworth, J. R.; Harrison, S. J.; Henderson, R. A.; Walton, D. R. M. *J. Chem. Soc., Chem. Commun.* **1984**, 176–177. (c) Dilworth, J. R.; Henderson, R. A.; Hills, A.; Hughes, D. L.; Macdonald, C.; Stephens, A. N.; Walton, D. R. M. *J. Chem. Soc., Dalton Trans.* **1990**, 1077–1085.
- (21) Schwindt, M.; Lejon, T.; Hegedus, L. S. *Organometallics* **1990**, *9*, 2814–2819.
- (22) Herrmann, W. A.; Salzer, A., Eds. *Synthetic Methods of Organometallics and Inorganic Chemistry*; Thieme: New York, 1996; Vol. 1, pp 47–48.

measurements were obtained by the method of Evans.²⁴ X-ray diffraction data were collected on a SMART6000 (Bruker) system under a stream of N₂(g) at low temperatures.²⁵ Synchrotron data were collected at the ChemMatCARS beamline (Argonne National Laboratory).

Synthesis of Complex 1 from NbCl₃(DME). To a thawing toluene suspension of NbCl₃(DME) (75 mg, 0.26 mmol) was added a thawing solution of Li(PNP) (113 mg, 0.26 mmol) in Et₂O. The resulting brown solution was allowed to warm to room temperature and stirred for 24 h. The solution was filtered, and volatiles were concentrated. Crystals were grown by layering the toluene solution with hexane and storing at -36 °C over several days. Alternatively, crystals may be grown at room temperature from Et₂O. Yield: 27%, 43 mg, 0.035 mmol. ¹H NMR (25 °C, 399.8 MHz, CD₂Cl₂): δ 7.36 (d, *Ar*, 2H), 7.01 (d, *Ar*, 2H), 6.92 (m, *Ar*, 4H), 6.69 (m, *Ar*, 2H), 6.46 (m, *Ar*, 2H), 3.789 (m, CH(CH₃)₂, 2H), 2.68 (septet, CH(CH₃)₂, 2H), 2.54 (septet, CH(CH₃)₂, 2H), 2.33 (s, ArCH₃, 6H), 2.30 (overlapped m, CH(CH₃)₂, 2H), 2.26 (s, ArCH₃, 6H), 1.67 (m, CH(CH₃)₂, 8), 1.60 (d, CH(CH₃)₂, 2), 1.37 (m, CH(CH₃)₂, 18H), 0.99 (dd, CH(CH₃)₂, 8H), 0.83 (m, CH(CH₃)₂, 6H), 0.45 (dd, CH(CH₃)₂, 6H). ¹³C{¹H} NMR (25 °C, 125.69 MHz, CH₂Cl₂): δ 159.1 (d, *Ar*), 157.5 (d, *Ar*), 133.5 (*Ar*), 132.1 (*Ar*), 131.9 (*Ar*), 131.6 (*Ar*), 131.1 (*Ar*), 130.1 (d, *Ar*), 128.5 (*Ar*), 123.1 (d, *Ar*), 119.7 (d, *Ar*), 117.7 (d, *Ar*), 27.1 (d, CHMe₂), 26.9 (d, CHMe₂), 25.3 (d, CHMe₂), 24.2 (d, CHMe₂), 21.3 (*ArMe*), 21.1 (d, CHMe₂), 20.9 (d, CHMe₂), 20.8 (*ArMe*), 20.6 (d, CHMe₂), 19.1 (d, CHMe₂), 18.8 (d, CHMe₂), 18.6 (d, CHMe₂), 16.2 (d, CHMe₂), 15.9 (d, CHMe₂). ³¹P{¹H} NMR (25 °C, 121.5 MHz, CH₂Cl₂): δ 47.08 (d, *J*_{P-P} = 96.2 Hz), 43.47 (d, *J*_{P-P} = 96.2 Hz). ¹⁵N NMR (23 °C, 50.7 MHz, CD₂Cl₂): δ 396.6. ⁹³Nb NMR (25 °C, 122.3 MHz, CD₂Cl₂): δ -3049 (br, Δ*ν*_{1/2} = 10 500 Hz). IR (solid, NaCl): 2963 (m), 2922 (m), 2861 (m), 1595 (w), 1526 (w), 1460 (s), 1256 (w), 1191 (w) cm⁻¹. Multiple attempts to obtain satisfactorily elemental analysis consistently yielded low percentage values in N content.

Synthesis of Complex 2. To a stirring, room-temperature suspension of NbCl₄(THF)₂ (100 mg, 0.396 mmol) in toluene was slowly added a toluene solution of Li(PNP) (172 mg, 0.396 mmol). The suspension gradually darkened over 1 h to form a purple solution. After stirring overnight, the solution was filtered and the solid washed thoroughly with toluene. The filtrate was reduced in vacuo to give a purple powder (213.8 mg, crude). Diffraction-quality crystals were grown from a room-temperature CH₂Cl₂ solution in an NMR tube. Yield: 69%, 172 mg, 0.274 mmol. ¹H NMR (25 °C, 399.8 MHz, C₆D₆): δ 12.36 (*ν*_{1/2} = 29.2 Hz), 5.63 (*ν*_{1/2} = 41.7 Hz), 3.90 (*ν*_{1/2} = 198.3 Hz), 3.68 (*ν*_{1/2} = 56.9 Hz), 3.48 (*ν*_{1/2} = 181.9 Hz), 2.84 (*ν*_{1/2} = 15.2 Hz), -6.16 (*ν*_{1/2} = 80.2 Hz), -12.19 (*ν*_{1/2} = 64.3 Hz). Magnetic moment, Evans' method: *μ*_{eff} = 1.79. X-band EPR (toluene, 25 °C): *I* = 1/2, 100%, [⁹³Nb] *A*_{iso} = 137 G, [³¹P] *A*_{iso} = 22 G, *g*_{iso} = 1.95. Elem anal. Calcd for C₂₆H₄₀NP₂NbCl₃: C, 49.70; H, 6.42; N, 2.23. Found: C, 49.40; H, 6.46; N, 2.19.

Synthesis of Complex 2-Cl. To a stirring toluene solution of **2** (144 mg, 0.23 mmol) was slowly added a THF solution of trityl chloride (Ph₃CCl; 64 mg, 0.23 mmol) at room temperature. The purple solution changed gradually to a green color after 2 h of stirring at 30 °C. After 6 h of stirring, the solvent was removed in

vacuo. The remaining solid was washed with hexane and -36 °C Et₂O and then dried to afford a green powder of **2-Cl** in 66% yield (101 mg, 0.15 mmol). The product was shown to be pure by ¹H and ³¹P{¹H} NMR spectra. Diffraction-quality crystals were grown from a benzene solution in an NMR tube at room temperature. ¹H NMR (25 °C, 300.1 MHz, C₆D₆): δ 6.94–6.50 (m, 6H, *Ar*), 2.91 (sept, 2H, CH(CH₃)₂), 2.58 (sept, 2H, CH(CH₃)₂), 2.11 (s, 6H, ArCH₃), 1.48 (dd, CH(CH₃)₂, 6H), 1.30 (dd, CH(CH₃)₂, 6H), 1.17 (dd, CH(CH₃)₂, 6H), 1.05 (dd, CH(CH₃)₂, 6H). ¹³C{¹H} NMR (25 °C, 100.6 MHz, CH₂Cl₂): δ 164.2 (d, *Ar*), 133.9 (*Ar*), 131.9 (*Ar*), 131.3 (*Ar*), 126.3 (d, *Ar*), 119.8 (d, *Ar*), 26.8 (d, CHMe₂), 26.6 (d, CHMe₂), 20.6 (CHMe₂), 19.8 (CHMe₂), 19.6 (CHMe₂), 19.4 (CHMe₂). ³¹P{¹H} NMR (25 °C, 121.5 MHz, C₆D₆): δ 75.7 (s). ⁹³Nb NMR (25 °C, 122.3 MHz, C₆D₆): δ -3091 (br, Δ*ν*_{1/2} = 9400 Hz). Multiple attempts to obtain satisfactorily elemental analysis were unsuccessful.

Synthesis of Complex 1 from the One-Electron Reduction of 2. Route A. To a thawing toluene solution of **2** (94 mg, 0.15 mmol) was slowly added a suspension of KC₈ (20 mg, 0.15 mmol) in toluene under an atmosphere of N₂. The stirring mixture gradually became brown after 1 h. After 24 h, solvent was removed in vacuo and the remaining powder was extracted with toluene. The solution was filtered and concentrated. Crystals of **1** were grown by layering the toluene solution with hexane and cooling to -36 °C. Yield: 23%, 21 mg, 0.017 mmol. ¹H and ³¹P{¹H} NMR spectra of the crystals were compared to those of samples prepared independently from NbCl₃(DME), N₂, and Li(PNP) (vide supra). **Route B.** To a thawing toluene solution of **2** (150 mg, 0.24 mmol) was slowly added a solution of HSnBu₃ (70 mg, 0.24 mmol) in hexane under an atmosphere of N₂. The stirring solution rapidly became red-brown, eventually changing to a purple solution after 3 h. After 6 h, the solvent was removed in vacuo, and the purple residue was washed thoroughly with hexane and cold Et₂O to afford **1** in pure form when judged by ¹H and ³¹P{¹H} NMR spectra. ¹H and ³¹P{¹H} NMR spectra of the solid were compared to those of samples prepared independently from NbCl₃(DME), N₂, and Li(PNP) (vide supra). Yield: 73%, 107 mg, 0.088 mmol.

Synthesis of Complex 1-¹⁵N₂. In a glovebox under an atmosphere of Ar, a toluene solution of **2** (200 mg, 0.32 mmol) was frozen in a three-necked round-bottomed flask. The flask was equipped with a vacuum adapter, a 100-mL bottle of ¹⁵N₂ with a break-seal, and a rubber septum. The round-bottomed flask was evacuated under vacuum, and ¹⁵N₂ was introduced into the flask after shattering the break-seal with the stirbar (using a magnet from outside of the flask). As the solution was allowed to thaw, a solution of HSnBu₃ (93 mg, 0.32 mmol) in pentane was slowly added via a syringe through the rubber septum. The stirring solution rapidly became red-brown, eventually changing to a purple solution after 3 h. After stirring for a total of 6 h, the solution was filtered and the solvent was removed in vacuo. The purple residue was washed thoroughly with hexane and cold Et₂O and then dried to afford **1** in pure form when judged by ¹H and ³¹P{¹H} NMR spectra. Yield: 69%, 134 mg, 0.11 mmol.

Synthesis of Complex 1 from [NbCl₃(THF)₂]₂(*μ*-N₂). To a -36 °C toluene solution of [NbCl₃(THF)₂]₂(*μ*-N₂) (500 mg, 0.70 mmol) was slowly added 2 equiv (608 mg, 1.40 mmol) of Li(PNP) in DME. After 3 h, a slight change in the shade of purple was observed. Following 6 h of stirring, the solvent was removed and the resulting purple solid was extracted with CH₂Cl₂. The solution was then filtered, and the filtrate was dried and washed thoroughly with hexane and dried under reduced pressure. The resulting purple powder was found to be free of major impurities by ¹H and ³¹P{¹H} NMR spectra. ¹H and ³¹P{¹H} NMR spectra of the solid

(23) ⁹³Nb NMR acquisition parameters were as follows: sw = 195599, at = 0.066, d1 = 0.500, decouple frequency 1 = 499.8 MHz [¹H], decouple frequency 2 = 50.65 MHz [¹⁵N].

(24) (a) Sur, S. K. *J. Magn. Reson.* **1989**, 82, 169–173. (b) Evans, D. F. *J. Chem. Soc.* **1959**, 2003–2005.

(25) (a) *SAINT 6.1*; Bruker Analytical X-ray Systems: Madison, WI. (b) *SHELXTL-Plus*, version 5.10; Bruker Analytical X-ray Systems: Madison, WI.

were compared to those of samples prepared independently from NbCl₃(DME), N₂, and Li(PNP) (vide supra). Crystals were grown from a room-temperature ethereal solution. The crystallographic unit cell was found to match that of the sample prepared from NbCl₃(DME), N₂, and Li(PNP). Yield: 88%, 746 mg, 0.616 mmol.

Synthesis of Complex 3. To a stirring suspension of NbCl₃(DME) (100 mg, 0.35 mmol) in toluene was added Li(PNP) (150 mg, 0.35 mmol). This suspension was allowed to stir for 5 min, and then a toluene solution of azobenzene (1 equiv) was added. The solution was stirred overnight at 30 °C, resulting in a brilliant purple solution. The solution was filtered and solvent removed in vacuo. The solid was washed thoroughly with hexane and then taken up into THF. Long, thin crystalline needles were grown by layering the THF solution with hexane. Yield: 89%, 241 mg, 0.311 mmol in multiple crops. ³¹P{¹H} NMR shows the presence of three isomeric forms. ³¹P{¹H} NMR (25 °C, 121.5 MHz, C₆D₆): δ 49.9 (d, ArN=P), 34.3 (br s, Nb–P), 47.8 (d, ArN=P), 37.1 (br s, Nb–P), 46.7 (d, ArN=P), 40.5 (br s, Nb–P). ¹H NMR (25 °C, 121.5 MHz, C₆D₆): δ 7.70–6.38 (m, Ar), 3.58 (THF), 2.72–1.96 (mixture of sept), 2.179 (s, ArCH₃), 2.146 (s, ArCH₃), 2.128 (s, ArCH₃), 2.10 (s, ArCH₃), 1.60–0.13 (CH(CH₃)₂), 1.39 (THF). Elem anal. Calcd for C₄₂H₅₈N₃Cl₂NbOP₂: C, 59.58; H, 6.90; N, 4.96. Found: C, 59.32; H, 7.28; N, 4.95.

General Parameters for Data Collection and Refinement. Single crystals of **1** (Et₂O), **2** (CH₂Cl₂), and **2-Cl** (C₆H₆) were grown at room temperature. Inert-atmosphere techniques were used to place the crystal onto the tip of a diameter glass capillary (0.1 mm) mounted on a SMART6000 (Bruker) at 112–128(2) K. A preliminary set of cell constants were calculated from reflections obtained from three nearly orthogonal sets of 20–30 frames. The data collection was carried out using graphite-monochromated Mo Kα radiation with a frame time of 10–60 s and a detector distance of 5.0 cm. A randomly oriented region of a sphere in reciprocal space was surveyed. Three sections of 606 frames were collected with 0.30° steps in ω at different φ settings with the detector set at –43° in 2θ. Final cell constants were calculated from the xyz centroids of strong reflections from the actual data collection after integration (SAINT).^{25a} The structure was solved in using SHELXS-97 and refined with SHELXL-97.^{25b} A direct methods solution was calculated that provided most non-H atoms from the E map. Full-matrix least-squares/difference Fourier cycles were performed that located the remaining non-H atoms. All non-H atoms were refined with anisotropic displacement parameters (unless otherwise mentioned). All H atoms were refined with isotropic displacement parameters (unless otherwise mentioned). Small single crystals of **3** (THF) were grown at –36 °C. The data collection was carried out using synchrotron radiation (λ = 0.495 95, diamond 111 monochromators, and two mirrors to exclude higher harmonics) with a frame time of 1 s and a detector distance of 5.0 cm. A randomly oriented region of reciprocal space was surveyed to the extent of approximately a hemisphere. One major section of frames was collected with 0.30° steps in ω and a detector position of 0° in 2θ. Data to a resolution of 0.80 Å were considered in the reduction. Final cell constants were calculated from the xyz centroids of 6288 strong reflections from the actual data collection after integration (SAINT).^{25a} The intensity data were corrected for absorption (SADABS).²⁶

Theoretical Studies. All calculations were carried out using density functional theory (DFT) as implemented in the Jaguar 5.5 suite²⁷ of ab initio quantum chemistry programs. Geometry

optimizations were performed with the B3LYP²⁸ functional and the 6-31G** basis set. Nb was represented using the Los Alamos LACVP** basis set, which includes relativistic effective core potentials.²⁹ The energies of the optimized structures were reevaluated by additional single-point calculations on each optimized geometry using Dunning's correlation-consistent triple-ζ basis set^{30c} cc-pVTZ(-f), which includes a double set of polarization functions. For Nb, a modified version of LACVP**, designated as LACV3P**, in which the exponents were decontracted to match the effective core potential with the triple-ζ basis set, was used. A simplified model was used to obtain Mayer's bond order³⁰ from NBO 5.013 implemented in the Jaguar 5.5 suite.

Results and Discussion

Treatment of Li(PNP)⁹ with NbCl₃(DME)¹⁸ over 24 h under a blanket of N₂ results in the formation of the diamagnetic, dinuclear, N₂ complex [(PNP)NbCl₂]₂(μ-N₂) (**1**) in 27% yield as black needles (Scheme 1). Compound **1** likely forms via a transient Nb(III) precursor “(PNP)NbCl₂”, which is trapped by molecular N₂. We speculate that formation of the hypothetical intermediate “(PNP)NbCl₂(N₂)” species is slow relative to generation of the (PNP)NbCl₂ precursor, which consequently results in the formation of the N₂-bridged dimer. The reaction must be performed under a bed of N₂; otherwise, a myriad of products are formed. To our knowledge, Fryzuk and co-workers have reported the only other example of N₂ activation by a group 5 metal without an external reductant and using a Nb(III) precursor.^{8f} In their studies, the dianionic pincer ligand NPN (NPN²⁻ = PhP(CH₂SiMe₂NPh)₂) and NbCl₃(DME) were treated under N₂ to generate a [(NPN)NbCl]₂(μ-N₂) system.^{8f}

Complex **1** is diamagnetic and has therefore been characterized by a combination of ¹H, ¹³C{¹H}, and ³¹P{¹H} NMR spectroscopy. The ¹H NMR spectrum of **1** is consistent with a centrosymmetric molecule in which each –N=NbCl₂–(PNP) fragment is equivalent. However, the twisting of the aryl groups on the pincer ligand renders each phosphine inequivalent; hence, two tolyl groups as well as four methine resonances are observed in the ¹H NMR spectrum. Likewise, the ³¹P{¹H} NMR spectrum of **1** is also consistent with two inequivalent phosphine groups (47 and 44 ppm), which are not significantly skewed from a strict “trans” geometry (*J*_{P–P} = 96 Hz). In addition to ¹H and ³¹P{¹H} NMR spectra, we were able to locate a broad resonance (–3049 ppm; Δ*ν*_{1/2} = 10 500 Hz) in the ⁹³Nb NMR spectrum of **1**.²³ Unfortunately, multiple attempts to locate an *ν*_{N–N} stretch in **1** or for the ¹⁵N₂ isotopomer [(PNP)NbCl₂]₂(μ-¹⁵N₂) (**1-¹⁵N₂**) were unsuccessful. We speculate that the centrosymmetric symmetry in **1** coupled with the weakness of the N–N bond might result in an obscured stretch. Gratifyingly, the ¹⁵N NMR

(28) (a) Becke, A. D. *Phys. Rev. A* **1988**, *38*, 3098. (b) Becke, A. D. *J. Chem. Phys.* **1993**, *98*, 5648. (c) Lee, C. T.; Yang, W. T.; Parr, R. G. *Phys. Rev. B* **1988**, *37*, 785. (d) Vosko, S. H.; Wilk, L.; Nusair, M. *Can. J. Phys.* **1980**, *58*, 1200.

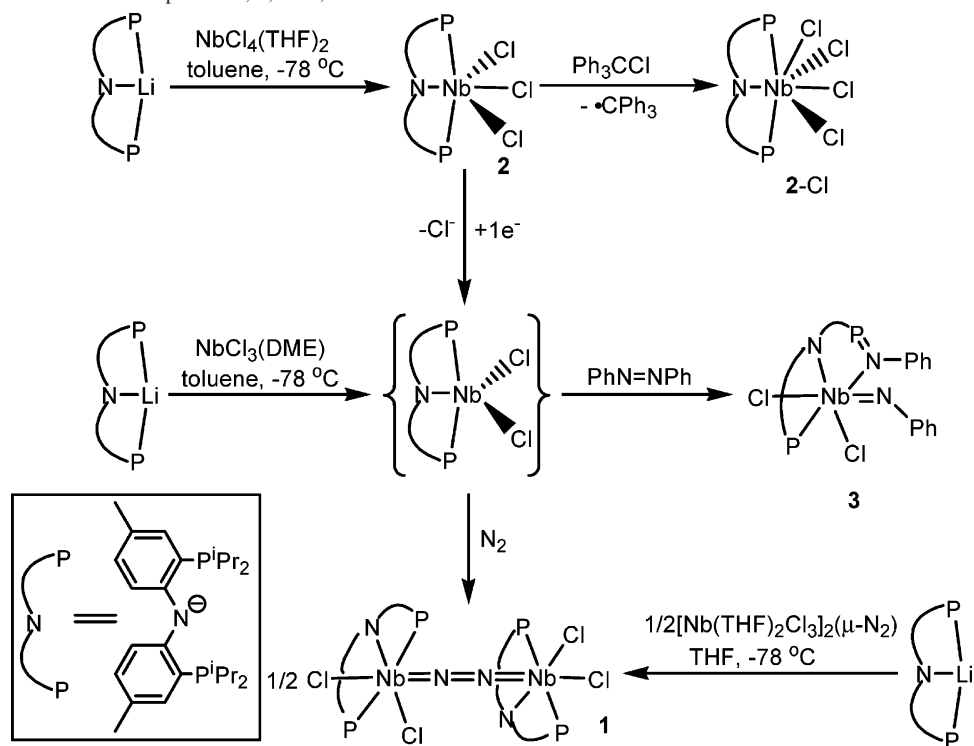
(29) (a) Hay, P. J.; Wadt, W. R. *J. Chem. Phys.* **1985**, *82*, 270. (b) Wadt, W. R.; Hay, P. J. *J. Chem. Phys.* **1985**, *82*, 284.

(30) (a) Mayer, I. *Chem. Phys. Lett.* **1983**, *97*, 270. (b) Mayer, I. *Int. J. Quantum Chem.* **1986**, *29*, 477. (c) Mayer, I. *Int. J. Quantum Chem.* **1986**, *29*, 73. (d) Bridgeman, A. J.; Cavigliasso, G.; Ireland, L. R.; Rothery, J. J. *Chem. Soc., Dalton Trans.* **2001**, 2095. (e) Dunning, T. H. *J. Chem. Phys.* **1989**, *90*, 1007.

(26) For, an empirical correction for absorption anisotropy, see: Blessing, R. *Acta Crystallogr.* **1995**, *A51*, 33–38.

(27) *Jaguar 5.5*; Schrödinger: Portland, OR, 1991–2003.

Scheme 1. Synthetic Routes to Compounds 1, 2, 2-Cl, and 3



spectrum of $1\text{-}^{15}\text{N}_2$ evinced a singlet at 396 ppm, thus hinting that the N's of the N_2 unit in complex **1** are symmetrically equivalent and that the formation of the N_2 bridge originates from atmospheric N_2 .

To address the degree of reduction in the N–N bond in **1**, we collected single-crystal X-ray diffraction data.³¹ Accordingly, the solid-state structure of **1** clearly reveals a dinuclear Nb complex possessing an end-on bridging N_2 ligand (Figure 1). Intensity statistics and systematic absences suggested the centrosymmetric tetragonal space group $I\bar{4}$, whereby each $\text{--N=NbCl}_2(\text{PNP})$ unit is symmetrically related. The Nb–N distance involving the N_2 ligand is evidently shorter [1.851(3) Å] than the typical Nb– N_{amide} distance [2.124(4) Å] in the pincer ligand and is thus consistent with the N_2 ligand having diimide character in **1**. Consequently, the N–N distance has been significantly increased [1.277(6) Å], thus suggesting that a resonance $(\text{PNP})\text{Nb}=\text{N}=\text{N}=\text{Nb}(\text{PNP})$ might be operative in **1** [Nb=

N–N, 172.8(2)°]. Each Nb center in the structure of **1** is confined in an octahedral environment, with the PNP framework occupying a meridional plane and the two chlorides being cis to each other.

A diimido complex similar to that of **1** was originally reported by Rocklage and Schrock^{20a} involving two Ta or Nb metal centers. Their work suggested that the N–N bond in N_2 was significantly reduced (at least by four electrons), rendering it a diimide ligand concurrent with a d^0 metal center. The Nb=N and N–N distances in compound **1** vary

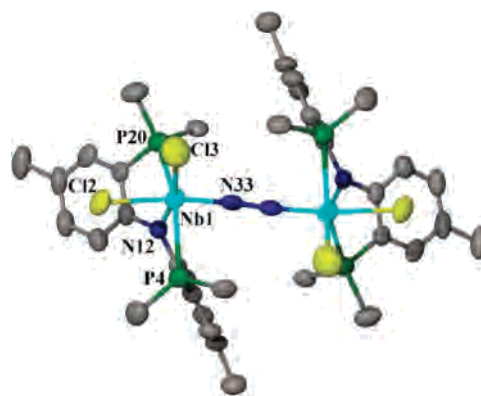


Figure 1. Molecular structure of complex **1** depicting thermal ellipsoids at the 50% probability level. H atoms, Pr methyls on P, and two Et_2O molecules have been excluded for clarity. Distances are reported in angstroms and angles in degrees. Selected metrical parameters: Nb1–N12, 2.124(4); Nb1–N33, 1.851(3); Nb1–P4, 2.623(4); Nb1–P20, 2.607(3); Nb1–Cl2, 2.502(3); Nb1–Cl3, 2.342(8); N33–N33', 1.277(6); P4–Nb1–P20, 147.14(5); Nb1–N33–N33', 172.8(2); N12–Nb1–N33, 97.3(4); N12–Nb1–Cl2, 86.6(1); N12–Nb1–Cl3, 161.8(1); N12–Nb1–P4, 72.3(1); N12–Nb1–P20, 74.8(1); N33–Nb1–P4, 100.5(1); N33–Nb1–P20, 84.4(1); N33–Nb1–Cl2, 169.7(1); N33–Nb1–Cl3, 96.6(1); Cl2–Nb1–Cl3, 81.70(6); Cl2–Nb1–P4, 89.69(4); Cl2–Nb1–P20, 87.55(5); Cl3–Nb1–P4, 93.63(5); Cl3–Nb1–P20, 118.28(6).

(31) Crystallographic details for $[(\text{PNP})\text{NbCl}_2]_2(\mu\text{-N}_2)(1)\cdot 2\text{Et}_2\text{O}$: A black needle of approximate dimensions $0.30 \times 0.30 \times 0.14 \text{ mm}^3$ was selected and mounted on a glass fiber. A total of 8320 reflections ($-22 < h < 22$, $-19 < k < 22$, $-31 < l < 31$) were collected at $T = 120(2) \text{ K}$ in the range of $2.36\text{--}27.51^\circ$, of which 5080 were unique ($R_{\text{int}} = 0.0681$); Mo $K\alpha$ radiation ($\lambda = 0.71073 \text{ \AA}$). A direct methods solution was calculated that provided most non-H atoms from the E map. All non-H atoms were refined with anisotropic displacement parameters. All H atoms were placed in ideal positions and refined as riding atoms with relative isotropic displacement parameters. Two crystallographically independent molecules and two disorder Et_2O solvent molecules were confined in the asymmetric unit. The residual peak and hole electron densities were $+0.770$ and -0.753 e/\AA^3 . The absorption coefficient was 0.588 mm^{-1} . The least-squares refinement converged normally with residuals of $R(F) = 0.0464$ and $wR(F^2) = 0.0836$ and a GOF = 0.815 [$I > 2\sigma(I)$]. $\text{C}_{56}\text{H}_{90}\text{Cl}_4 \text{Nb}_2\text{OP}_4$, space group $I\bar{4}$, tetragonal, $a = 17.2449(7) \text{ \AA}$, $b = 17.2449(7) \text{ \AA}$, $c = 24.280(2) \text{ \AA}$, $\alpha = \beta = \gamma = 90^\circ$, $V = 7220.5(8) \text{ \AA}^3$, $Z = 4$, $D_{\text{calc}} = 1.184 \text{ mg/m}^3$, $F(000) = 2688$.

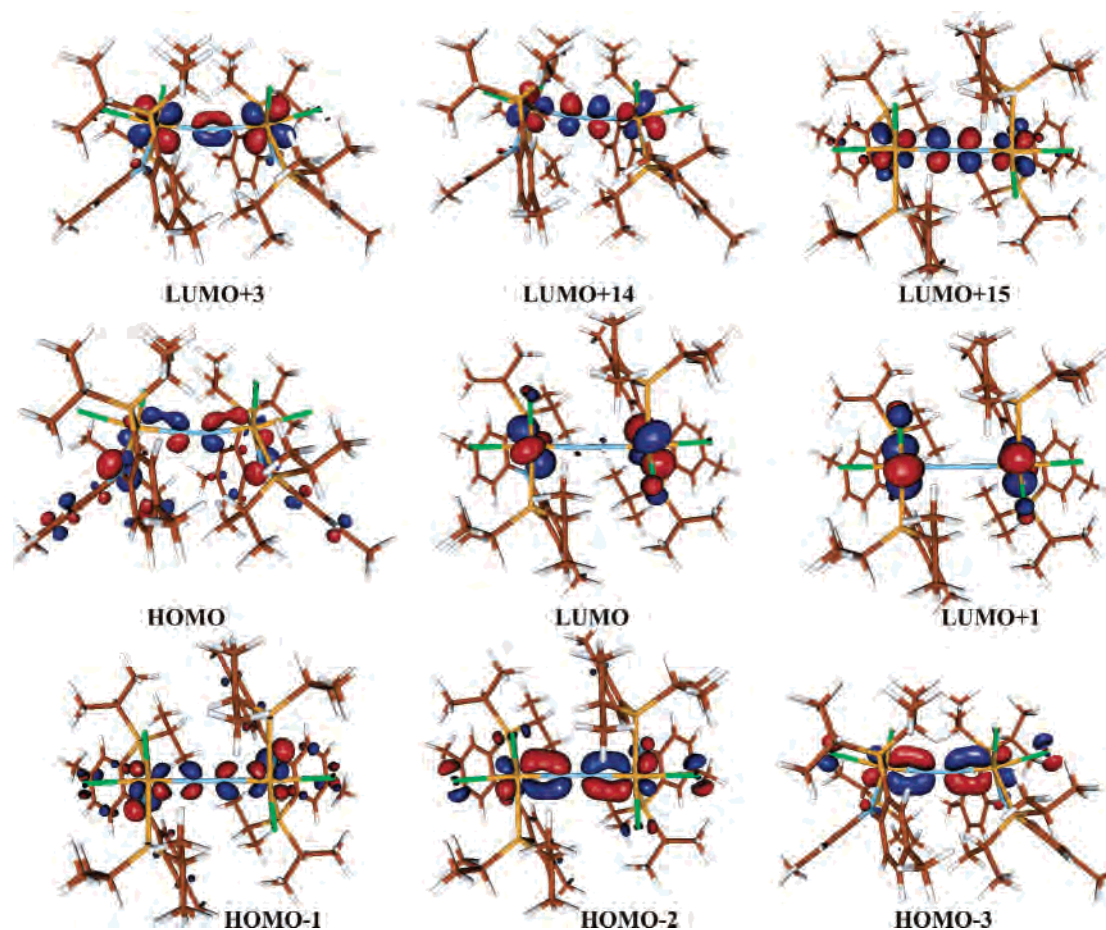


Figure 2. Selected molecular orbitals for the full model of complex **1**.

significantly from the metrical parameters reported for the $Nb=N-N=Nb$ core of Gambarotta's $[(C_2N)_3Nb]_2(\mu-N_2)$ [Cy = *cyclo*- C_6H_{11} ; $Nb=N$, 1.812(6) Å; $N-N$, 1.34(1) Å]^{14a} and Floriani's calixarene system $[Na(solvent)]_2\{[(calixarene)-Nb]_2(\mu-N_2)\}$ [donor solvent = THF, diglyme, DME, 18-crown-6; calixarene⁴⁻ = *p*-^tBu-calix⁴arene-(O)₄; $Nb=N$, 1.75(2) Å; $N-N$, 1.39(7) Å].^{14b,c} However, our metrical parameters ($Nb=N$ and $N-N$ distances) are comparable to Fryzuk's $[(P_2N_2)Nb]_2(\mu-N_2)$ ($P_2N_2^{2-}$ = $PhP(CH_2SiMe_2NSiMe_2CH_2)PPh$) [$Nb=N$, ~1.85 Å; $N-N$, 1.272(5) Å]^{12d} and $[(NPN)NbCl]_2(\mu-N_2)$ [$Nb=N$, 1.843(2) Å; $N-N$, 1.273(4) Å]^{8f} related molecules.

Computational studies on the full model of **1** suggest that the frontier orbitals are located primarily on the Nb center and NbN_2Nb unit. Evidence for π bonding about the NbN_2Nb core in **1** is corroborated by two orthogonal π -bonding interactions, HOMO-2 and HOMO-3 (Figure 2). While the highest occupied molecular orbital (HOMO) appears to involve some $Nb=N$ π bonding augmented by a N lone pair from the PNP pincer framework. The lowest unoccupied molecular orbital (LUMO) and LUMO+1 are essentially nonbonding metal-based orbitals with some minor $Nb-Cl$ π^* contribution (Figure 2). Although the former orbitals suggest that reduction of **1** would result in the formation of Nb(IV) and the weakening of the Cl^- ligand, the HOMO-LUMO gap (~2.4 eV) implies that such a process would be high in energy. Antibonding orbitals such as LUMO+3,

LUMO+14, and LUMO+15 also indicate that the NbN_2Nb core in **1** would not be perturbed upon reduction because population of these orbitals would be highly unlikely. Judging from the nature of the frontier and near-frontier orbitals, it appears that the reduction of **1** by $2e^-$ would not result in $N-N$ splitting. In fact, attempts to perform a chemical reduction of **1** with reagents such as KC_8 , $Mg((THF)_3\text{-anthracene})$, $Na(C_{10}H_8)$, Na/Hg , and Bu_3SnH have resulted in decomposition mixtures or no reaction.

Because spin states other than a singlet ground state are conceivable for **1**, geometry optimizations were carried out for singlet, triplet, and quintet spin states. The lowest self-consistent-field energy [$E(SCF)$] was found to be the singlet state by at least ~20 kcal/mol (see the Supporting Information). This also provides further evidence for a $2e^-$ reduction of N_2 by each Nb center. To gain additional insight into the bonding of the NbN_2Nb core, Mayer bond orders³⁰ were computed for the $Nb=N$ and $N-N$ linkages. Each $Nb=N_{diimide}$ bond was found to have a bond order of 1.3, supporting the assignment of a double bond. Likewise, the $N-N$ bond order was found to be 1.5, suggesting that reduction from that of free N_2 (2.8) has occurred. Hence, these results imply that bonding at the core of complex **1** most likely lies between the topologically linear $Nb=N=N=Nb$ and $Nb=N-N=Nb$ cores.

Despite our success in isolating **1** from N_2 , formation of such a product from the niobium(III) halide precursor was

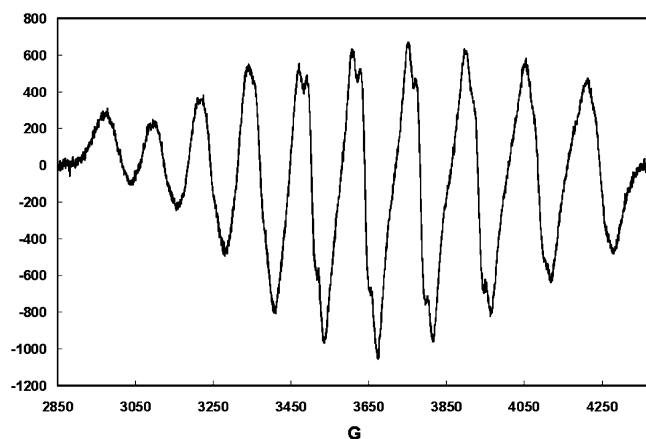


Figure 3. Isotropic X-band solution EPR spectrum of complex **2** recorded in toluene (206 μ M). Acquisition parameters: frequency = 9.439 088 GHz, MF = 100 kHz, MA = 11 G, P = 0.2008 mW.

not clean, consequently resulting in a low yield of pure product. Hence, a modified protocol to the formation of **1** was pursued.

Accordingly, when $\text{NbCl}_4(\text{THF})_2$ ¹⁹ is swiftly added to a cold solution of Li(PNP) in toluene at -36 °C, purple (PNP)- NbCl_3 (**2**) is isolated in 86% yield (Scheme 1). Complex **2** is a d^1 paramagnet; hence, the electron paramagnetic resonance (EPR) spectrum displays a classic 10-line pattern resulting from coupling of the unpaired electron to the Nb ($I = 1/2$, 100%, $[\text{Nb}]A_{\text{iso}} = 137$ G; Figure 3). Fortunately, superhyperfine coupling to the proximal P atoms was partially resolved ($[\text{P}]A_{\text{iso}} = 22$ G, $g_{\text{iso}} = 1.95$; Figure 3). However, formation of **2** was marred by the significant content of another material, which we have been unable to identify. We were, however, able to obtain satisfactorily elemental analysis and reliable solution magnetization measurements such as an Evans from a small fraction of crystallized product (low yield).²⁴

To elucidate an accurate connectivity map in paramagnetic **2**, we collected single-crystal X-ray diffraction data (Figure 4).³² As speculated, the molecular structure of **2** reveals a monomeric Nb(IV) center confined in a slightly distorted octahedral environment. All Nb–Cl distances are within the range for typical Nb(IV)–Cl ligands,^{5c,t} and the Nb– N_{amide} and Nb– $P_{\text{phosphine}}$ distances are comparable to the metrical parameters observed in the solid-state structure of **1**. Because of the rigid pincer-type coordination imposed by the ligand, the three remaining Cl atoms in **2** are dispersed along the

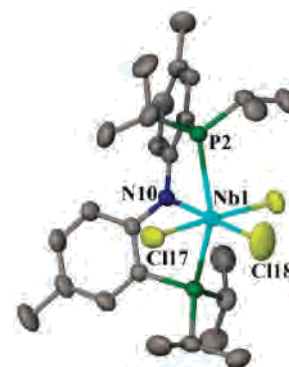


Figure 4. Molecular structure of complex **2** depicting thermal ellipsoids at the 50% probability level. H atoms have been excluded for clarity. Distances are reported in angstroms and angles in degrees. Selected metrical parameters: Nb1–N10, 2.085(3); Nb1–P2, 2.6057(6); Nb1–Cl17, 2.4031(6); Nb1–Cl18, 2.363(2); P2–Nb1–P2', 149.00(3); Cl17–Nb1–Cl17', 175.08(4); P2–Nb1–N10, 74.50(5); P2–Nb1–Cl17, 90.54(2); P2–Nb1–Cl18, 105.50(5); N10–Nb1–Cl17, 92.46(2); N10–Nb1–Cl18, 180.000(1); Cl17–Nb1–Cl18, 87.54(2).

mer plane. The solid-state structure of **2** displays no other exceptional features.

To assess the bulk purity of **2**, we carried out its one-electron oxidation using ClCPh_3 in toluene, which produced the diamagnetic complex (PNP) NbCl_4 (**2-Cl**; 66% isolated yield; Scheme 1). ^1H , $^{31}\text{P}\{^1\text{H}\}$, $^{13}\text{C}\{^1\text{H}\}$, and ^{93}Nb NMR data unambiguously confirm a Nb(V) system resulting from oxidation with $^+\text{CPh}_3$. Congruently, the spectroscopic observation of Gomberg's dimer³³ in the ^1H NMR solution mixture is also consistent with a redox reaction taking place. Despite the fact that the Nb species might be seven-coordinate, the $^{31}\text{P}\{^1\text{H}\}$ NMR spectrum is undeviating with a highly symmetric complex where both phosphines composing the pincer ligand are equivalent (75.7 ppm). Likewise, the ^1H NMR spectrum of **2-Cl** reveals only one tolyl methyl resonance (2.11 ppm), as well as two isopropyl methine resonances (2.91 and 2.58 ppm). Each isopropyl group reveals diastereotopic isopropyl methyl resonances, thus indicative of the complex having C_2 symmetry in solution. As expected, the ^{93}Nb NMR spectrum of **2-Cl** (-3091 , $\Delta\nu_{1/2} = 9400$ Hz) is in agreement with a diamagnetic Nb complex resulting from a one-electron oxidation.

To ascertain whether the Nb(V) ion in **2-Cl** has a coordination number of seven, we collected solid-state crystal data. Accordingly, the molecule structure of **2-Cl** depicts a seven-coordinate Nb(V) confined between a capped octahedron and a capped trigonal prism environment (Figure 5).³⁴ Looking down the Cl133–Cl134 axis in **2-Cl**, it appears as if the geometry could also be that of a highly distorted pentagonal bipyramid. However, the Cl133–Nb1–Cl134 angle of 163.99° is deviated from true linearity, and we refrain from classifying **2-Cl** as a pentagonal bipyramid because none of the atoms composing the first coordination sphere at Nb are strictly trans to each other. We speculate that the rigidity of the PNP ligand seems to prevent the molecule from adopting any well-defined geometry for a mononuclear seven-coordinate system. In the structure of

(32) Crystallographic details for (PNP) NbCl_3 (**2**): A dark irregular crystal of approximate dimensions $0.12 \times 0.12 \times 0.10$ mm³ was selected and mounted on a glass fiber. A total of 3389 reflections ($-13 < h < 15$, $-12 < k < 12$, $-17 < l < 17$) were collected at $T = 128(2)$ K in the range of 2.21 – 27.57° , of which 2517 were unique ($R_{\text{int}} = 0.0489$); Mo $K\alpha$ radiation ($\lambda = 0.71073$ Å). A direct methods solution was calculated that provided most non-H atoms from the E map. All non-H atoms were refined with anisotropic displacement parameters. All H atoms were placed in ideal positions and refined as riding atoms with relative isotropic displacement parameters. The residual peak and hole electron densities were $+0.429$ and -0.422 e/Å³. The absorption coefficient was 0.809 mm⁻¹. The least-squares refinement converged normally with residuals of $R(F) = 0.0295$ and $wR(F^2) = 0.0577$ and a GOF = 0.887 [$I > 2\sigma(I)$]. $\text{C}_{26}\text{H}_{40}\text{Cl}_3\text{NNbP}_2$, space group $P2_1/n$, monoclinic, $a = 11.639(3)$ Å, $b = 9.673(1)$ Å, $c = 13.126(4)$ Å, $\beta = 97.165(3)^\circ$, $V = 1466.2(3)$ Å³, $Z = 2$, $D_{\text{calc}} = 1.422$ mg/m³, $F(000) = 650$.

(33) (a) Gomberg, M. *J. Am. Chem. Soc.* **1900**, 22, 757–771. (b) McBride, J. M. *Tetrahedron* **1974**, 30, 2009–2022.

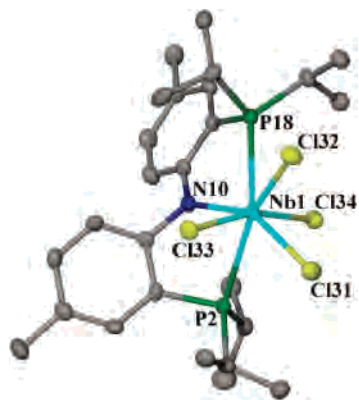


Figure 5. Molecular structure of complex **2-Cl** depicting thermal ellipsoids at the 50% probability level. H atoms and the solvent have been excluded for clarity. Distances are reported in angstroms and angles in degrees. Selected metrical parameters: Nb1–N10, 2.126(3); Nb1–P2, 2.700(1); Nb1–P18, 2.636(1); Nb1–Cl31, 2.470(1); Nb1–Cl32, 2.430(1); Nb1–Cl33, 2.3677(9); Nb1–Cl34, 2.369(1); P2–Nb1–P18, 137.14(3); P2–Nb1–N10, 70.88(8); P2–Nb1–Cl31, 77.39(3); P2–Nb1–Cl32, 152.62(3); P2–Nb1–Cl33, 82.11(3); P2–Nb1–Cl34, 82.65(3); P18–Nb1–N10, 71.42(8); P18–Nb1–Cl31, 138.81(3); P18–Nb1–Cl32, 70.21(3); P18–Nb1–Cl33, 113.93(3); P18–Nb1–Cl34, 80.86(3); N10–Nb1–Cl31, 148.15(8); N10–Nb1–Cl32, 132.84(8); N10–Nb1–Cl33, 84.88(8); N10–Nb1–Cl34, 94.73(8); Cl31–Nb1–Cl32, 77.45(3); Cl31–Nb1–Cl33, 88.19(3); Cl31–Nb1–Cl34, 83.73(4); Cl32–Nb1–Cl33, 86.47(3); Cl32–Nb1–Cl34, 105.12(4); Cl33–Nb1–Cl34, 163.99(3).

2-Cl, the Cl atoms pseudotrans to the phosphine and amide donors (Cl132 and Cl131) are elongated when compared to the trans Cl atoms (Cl133 and Cl134). As opposed to **2**, the greater coordination environment in **2-Cl** renders the P–Nb–P angle more acute [137.14(3)°].

As opposed to oxidation, we have discovered that complex **2** can be treated with one-electron reductants such as KC₈²¹ or Bu₃SnH in toluene, to provide compound **1** in 23 and 73% yield, respectively. Other reductants such as Na, Na/Hg, and Mg(THF)₃(anthracene)²² failed to improve the yield of **1**. Replacement of the harsh alkali metal for a more soluble and milder reductant such as tin hydride greatly improved the overall yield of **1**. Therefore, we propose that the formation of **1** from the one-electron reduction of **2** involves, again, generation of a transient Nb(III) intermediate “(PNP)-NbCl₂” (Scheme 1), which undergoes sequestration of molecular nitrogen to furnish the N₂-containing product.

However, our best approach to the NbN₂Nb scaffold bearing the PNP ligand was an independent reaction involving salt metathesis of Li(PNP) with Rocklage and Schrock^{20a}

(34) Crystallographic details for (PNP)NbCl₄ (**2-Cl**)·½C₆H₆: A green irregular crystal of approximate dimensions 0.25 × 0.25 × 0.20 mm³ was selected and mounted on a glass fiber. A total of 7312 reflections (–22 < h < 22, –12 < k < 12, –24 < l < 24) were collected at T = 120(2) K in the range of 2.12–27.54°, of which 4278 were unique (R_{int} = 0.0984); Mo Kα radiation (λ = 0.710 73 Å). A direct methods solution was calculated that provided most non-H atoms from the E map. All non-H atoms were refined with anisotropic displacement parameters. All H atoms were placed in ideal positions and refined as riding atoms with relative isotropic displacement parameters. A benzene solvent is present on a two-fold axis. The residual peak and hole electron densities were +1.063 and –0.806 e/Å³. The absorption coefficient was 0.838 mm^{–1}. The least-squares refinement converged normally with residuals of R(F) = 0.0395 and wR(F²) = 0.0735 and a GOF = 0.836 [I > 2σ(I)]. C₂₉H₄₃Cl₄NNbP₂, space group P2₁/c, monoclinic, a = 17.362(9) Å, b = 9.589(1) Å, c = 19.127(2) Å, β = 95.152(3)°, V = 3171.5(6) Å³, Z = 4, D_{calcd} = 1.471 mg/m³, F(000) = 1452.

and Henderson’s complex [NbCl₃(THF)₂]₂(μ-N₂)^{20b,c} (88% yield; Scheme 1). This route obviously makes incorporation of the ¹⁵N-enriched N₂^{4–} difficult because the precursor [NbCl₃(THF)₂]₂(μ-N₂) is not prepared from atmospheric N₂ but either by Wittig chemistry using the azine PhCH=N–N=CHPh and Nb=CH^tBu(THF)₂Cl₃^{20a} or from trimethylsilyl chloride elimination applying NbCl₅ and the hydrazine (Me₃Si)₂N–N(SiMe₃)₂.^{20b,c} Regardless of this limitation, our previous protocols (vide supra) to **1** from N₂ activation provide a convenient approach to at least 98% ¹⁵N enrichment, which is not the case for the latter method.

Multiple attempts to isolate putative “(PNP)NbCl₂” under Ar failed. We found, however, that treatment of NbCl₃(DME) with Li(PNP) in toluene, under Ar, followed by the addition of azobenzene resulted in the formation of a diamagnetic material. The order of addition of reagents has no impact on the outcome of the reaction. Congruently, when NbCl₃(DME) was treated with azobenzene, no reaction was evident, thus hinting that transmetalation of the niobium(III) halide precursor with Li(PNP) was likely the first step in the former reaction. The ¹H NMR spectrum of the new product revealed broad resonances in the aryl and aliphatic regions, while the ³¹P{¹H} NMR spectrum clearly showed two major P resonances at 47 and 41 ppm. However, in addition to the two major resonances, two more sets of signals were observed in the ³¹P{¹H} NMR spectrum, thus suggesting that a total of three species were likely present in solution. Multiple attempts to separate the three products by fractional crystallization were unsuccessful, while the elemental analysis of the crystalline material was consistent with the proposed formula C₄₂H₅₈N₃Cl₂NbOP₂ (approximately 1 equiv of THF was observed by ¹H NMR for EA samples). This suggested that the resonances observed in the ³¹P{¹H} NMR spectrum could be the result of isomers being present.

Given the ambiguity of both the ¹H and ³¹P{¹H} NMR spectra of the new product(s) and to ascertain the correct connectivity of this complex, it was necessary to collect crystal X-ray diffraction data of small needles using a synchrotron radiation source.³⁵ To our surprise, the solid-state crystal structure exposes a coordinatively saturated Nb(V) system (PNP=NPh)Nb=NPhCl₂ (**3**) (PNP=NPh[–] =

(35) Crystallographic details for (PNP=NPh)Nb=NPhCl₂ (**3**)·3.5THF: A purple irregular crystal of approximate dimensions 0.06 × 0.02 × 0.02 mm³ was selected and mounted on a glass fiber. A total of 20 738 reflections (–23 < h < 23, –13 < k < 13, –25 < l < 30) were collected at T = 173(2) K in the range of 0.59–18.05°, of which 15 832 were unique (R_{int} = 0.0792); synchrotron radiation (λ = 0.495 95 Å, diamond 111 monochromators, two mirrors to exclude higher harmonics). A direct methods solution was calculated that provided most non-H atoms from the E map. All non-H atoms were refined with anisotropic displacement parameters. All H atoms were placed in ideal positions and refined as riding atoms with relative isotropic displacement parameters. Restraints were employed in modeling the solvent molecules, which were refined isotropically. Two crystallographically independent molecules were confined in the asymmetric unit. The residual peak and hole electron densities were +1.982 and –2.270 e/Å³. The absorption coefficient was 0.802 mm^{–1}. The least-squares refinement converged normally with residuals of R(F) = 0.0898 and wR(F²) = 0.2345 and a GOF = 1.047 [I > 2σ(I)]. C₅₂H₇₈Cl₂N₃NbO_{3.50}P₂, space group P2₁(1), monoclinic, a = 18.46(1) Å, b = 12.192(8) Å, c = 24.40(1) Å, β = 99.90(9)°, V = 5408(5) Å³, Z = 4, D_{calcd} = 1.261 mg/m³, F(000) = 2176.

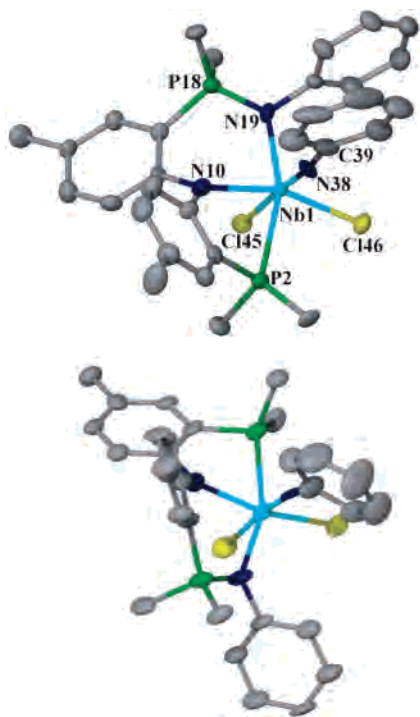
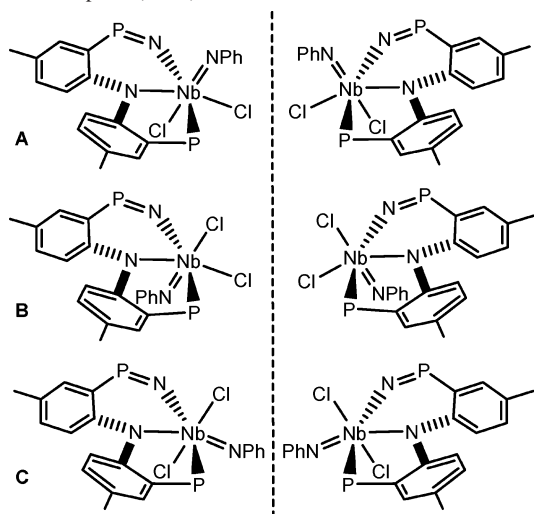


Figure 6. Molecular structure of complex **3** depicting thermal ellipsoids at the 50% probability level. Isopropyl methyls on P and H atoms and THF molecules have been excluded for clarity. The two crystallographically independent molecules (but chemically equivalent and non-superimposable) in the asymmetric unit are depicted. Distances are reported in angstroms and angles in degrees for the top isomer only. Selected metrical parameters: Nb1–N38, 1.788(8); Nb1–N19, 2.136(7); Nb1–N10, 2.140(7); Nb1–Cl46, 2.454(2); Nb1–Cl45, 2.575(2); Nb1–P2, 2.642(3); N19–P18, 1.632(7); Nb1–N38–C39, 172.8(7); N38–Nb1–Cl45, 177.2(3); N38–Nb1–N19, 95.2(3); N38–Nb1–N10, 95.3(3); N38–Nb1–Cl46, 94.6(3); N38–Nb–P2, 88.4(2); N19–Nb1–Cl46, 109.8(8); N19–Nb1–N10, 86.5(3); N19–Nb1–Cl45, 87.5(2); N19–Nb1–P2, 159.1(8); N10–Nb1–Cl45, 85.6(2); N10–Nb1–Cl46, 160.0(2); N10–Nb1–P2, 72.7(9); Cl45–Nb1–Cl46, 83.80(8); Cl45–Nb1–P2, 89.28(8); P2–Nb1–Cl46, 90.30(8).

$\text{N}[2\text{-P}(\text{CHMe}_2)_2\text{-4-methylphenyl}][2\text{-P}=\text{NPh}(\text{CHMe}_2)_2\text{-4-methylphenyl}]$ bearing a terminal phenylimide ligand $[\text{Nb}=\text{N}, 1.788(8) \text{ \AA}]$; Figure 6]. In the asymmetric unit, two crystallographically independent molecules are present along with seven THF solvent molecules. Each Nb molecule contains a $\text{Nb}=\text{N}_{\text{imide}}$ linkage in a nominally axial position with all N atoms in an effective *fac* orientation. However, the spatial position of the phosphoranimine, the skewing of the diaryl backbone for the PNP=NPh ligand (C_1 symmetric), and the orientation of the imide functionality render these two crystallographic isomers non-superimposable. Because the imide group can occupy three different sites, three distinct isomeric forms are possible (A–C, Chart 1). Consequently, each structure could contain mirror images, which would result in a total of six possible configurations for complex **3** (Chart 1). The solid-state structure of **3** reveals only two of the isomers having the phenylimide group trans to the chloride and not the PNP=NPh amide group (forms A and B). From our $^{31}\text{P}\{\text{H}\}$ NMR data however (vide supra), we believe that at least three of the possible isomers are observed spectroscopically. Another salient crystallographic feature in the structure of **3** worth mentioning is the $\text{P}=\text{N}$ distance [1.632(7) \AA], which is consistent with ylide formation. The latter functional group results in coordination of the nucleo-

Chart 1. Three Possible Isomeric Forms Generated from Azobenzene N=N Bond Rupture (A–C)^a



^a Possible enantiomeric forms are depicted to the right. The ^iPr groups on the P atoms and phenyl rings on the phosphoranimine N have been omitted for the purpose of clarity.

philic phosphoranimine N to the Nb(V) metal center $[\text{Nb1}-\text{N19}, 2.136(7) \text{ \AA}]$.³⁶ Relevant metrical parameters for one of the isomers are reported in Figure 6.

The formation of **3** likely occurs via the cooperative four-electron reduction of azobenzene by both Nb(III) and P(III) centers. Fryzuk and co-workers have observed relatively similar insertion reactions of metal nitrides (originated from N_2) into the phosphine atoms composing the supporting ancillary ligand.³⁸ In our case, azobenzene cleavage could result from this reagent adding across the Nb–P linkage, followed by subsequent electron shuffling to form the niobium phenylimide ($\text{Nb}=\text{NPh}$) and phosphoranimine ($\text{P}=\text{NPh}$) groups. However, compound **3** could also be generated via a Nb(V) η^2 -azobenzene intermediate “(PNP)NbCl₂(η^2 -

(36) For an example of a phosphoranimine-based ligand coordinated to an early transition metal, see: Cavell, R. G.; Kamalesh Babu, R.; Kasani, A.; McDonald, R. *J. Am. Chem. Soc.* **1999**, *121*, 5805–5806.

(37) For examples of azobenzene N=N bond cleavage reactions, see: (a) Wigley, D. E. *Prog. Inorg. Chem.* **1994**, *42*, 239–482. (b) Lockwood, M. A.; Fanwick, P. E.; Eisenstein, O.; Rothwell, I. P. *J. Am. Chem. Soc.* **1996**, *118*, 2762–2763. (c) Diaconescu, P. L.; Arnold, P. L.; Baker, T. A.; Mendiola, D. J.; Cummins, C. C. *J. Am. Chem. Soc.* **2000**, *122*, 6108–6109. (d) Warner, B. P.; Scott, B. L.; Burns, C. J. *Angew. Chem., Int. Ed.* **1998**, *37*, 959–960. (e) Gray, S. D.; Thorman, J. L.; Adamian, V. A.; Kadish, K. M.; Woo, L. K. *Inorg. Chem.* **1998**, *37*, 1–4. (f) Smieja, J. A.; Gozum, J. E.; Gladfelter, W. L. *Organometallics* **1987**, *6*, 1311–1317. (g) Zambrano, C. H.; Fanwick, P. E.; Rothwell, I. P. *Organometallics* **1994**, *13*, 1174–1177. (h) Schrock, R. R.; Glassman, T. E.; Vale, M. G.; Kol, M. *J. Am. Chem. Soc.* **1993**, *115*, 1760–1772. (i) Peters, R. G.; Warner, B. P.; Burns, C. J. *J. Am. Chem. Soc.* **1999**, *121*, 5585–5586. (j) Aubart, M. A.; Bergman, R. G. *Organometallics* **1999**, *18*, 811–813. (k) Barry, J. T.; Chisholm, M. H.; Foltling, J. M.; Huffman, J. C.; Streib, W. E. *Polyhedron* **1997**, *16*, 2113–2133. (l) Hill, J. E.; Profflet, R. D.; Fanwick, P. E.; Rothwell, I. P. *Angew. Chem., Int. Ed. Engl.* **1990**, *29*, 664–665. (m) Hansert, B.; Vahrenkamp, H. *J. Organomet. Chem.* **1993**, *459*, 265–269. (n) Smith, J. M.; Lachicotte, R. J.; Holland, P. L. *J. Am. Chem. Soc.* **2003**, *125*, 15752–15753. (o) Evans, W. J.; Drummond, D. K. *J. Am. Chem. Soc.* **1986**, *108*, 7440–7441. (p) Evans, W. J.; Drummond, D. K.; Chamberlain, L. R.; Doedens, R. J.; Bott, S. G.; Zhang, H.; Atwood, J. L. *J. Am. Chem. Soc.* **1988**, *110*, 4983–4994. (q) Ohki, Y.; Takikawa, Y.; Hatanaka, T.; Tatsumi, K. *Organometallics* **2006**, *25*, 3111–3113. (r) Nakajima, Y.; Suzuki, H. *Organometallics* **2005**, *24*, 1860–1866. (s) Komura, T.; Matsuo, T.; Kawaguchi, H.; Tatsumi, K. *Inorg. Chem.* **2005**, *44*, 175–177.

PhNNPh)", which would subsequently undergo nitrene group transfer to P to form the corresponding ylide.

Regardless of what mechanism might be operative, it is lucid that the creation of **3** involves a Nb(III) precursor, which in cooperation with the adjacent P(III) atom reduces the N=N bond of azobenzene. This implies that both Nb(III) and P(III) must each be contributing two electrons in order to make this reaction plausible. Azobenzene cleavage to form a phenylimide complex has been documented.³⁷ However, examples of cooperative and heteronuclear N=N splitting of azobenzene is, to the best of our knowledge, a rare type of transformation.^{37s}

Conclusions

In summary, we have shown that a dinuclear N₂ complex of Nb can be prepared via the activation of N₂ with a Nb(III) precursor and without the use of an external reductant. N₂ sequestration can also be achieved by one-electron reduction of a Nb(IV) starting material or by salt metathesis using a dinuclear Nb(V) having an end-on bridging N₂ scaffold. On the basis of X-ray and DFT analysis, the N₂ complex reported in this work is best described as a diimido ligand bridging two Nb(V) metal centers. When using reagents such as NbCl₃(DME) or NbCl₄(THF)₂, the dinuclear N₂ complex generated from these precursors likely proceeds by the formation of a reactive Nb(III) complex, which subsequently traps N₂ by a dinuclear, four-electron reduction process. Further evidence for the putative Nb(III) species

being a powerful multielectron reductant stems from its reaction with azobenzene to form a Nb=NPh linkage. However, in the latter case, oxidation of the P ligand also ensues, thus completely cleaving the N=N bond in azobenzene in an overall four-electron, cooperative, reduction process. Our inability to isolate the elusive complex "(PNP)-NbCl₂" in the absence of traps N₂ or azobenzene infers that the pincer-type ligand framework discussed in this work is likely an insufficiently robust ligand to stabilize a potent Nb(III) ion. We are currently examining the chemistry of a system such as **1** because its diimide moiety, generated from N₂ reduction, might be prone to group transfer reactions.^{12d}

Acknowledgment. We thank the Dreyfus Foundation, the Alfred P. Sloan Foundation, the Camille and Henry Dreyfus Foundation (Teacher–Scholar Award to D.J.M.), and the NSF (Grant CHE-0348941, PECASE to D.J.M.) for financial support of this research. ChemMatCARS Sector 15 is principally supported by the National Science Foundation/Department of Energy under Grant CHE0087817. The Advanced Photon Source is supported by the U.S. Department of Energy, Basic Energy Sciences, Office of Science, under Contract W-31-109-Eng-38. The authors thank Dr. Maren Pink for collecting synchrotron data and Professor C. Cummins and Nick Piro for insightful discussions.

Supporting Information Available: Complete crystallographic data (complexes **1**, **2**, **2-Cl**, and **3**), theoretical data (**1**), and experimental data (NMR data for compounds **1** and **2-Cl**). This material is available free of charge via the Internet at <http://pubs.acs.org>.

(38) Morello, L.; Yu, P.; Carmichael, C. D.; Patrick, B. O.; Fryzuk, M. D. *J. Am. Chem. Soc.* **2005**, *127*, 12796–12797.

IC061642B